Carbohydrate Polymers 95 (2013) 100–106

Contents lists available at SciVerse ScienceDirect

Carbohydrate Polymers

journal homepage: www.elsevier.com/locate/carbpol

Thermo-mechanical properties of the composite made of poly (3-hydroxybutyrate-co-3-hydroxyvalerate) and acetylated chitin nanocrystals

Bingjie Wang[a], Jun Li[b], Jianqiang Zhang[a,c], Huyan Li[a], Peng Chen[a], Qun Gu[a,*], Zongbao Wang[a,**]

[a] Ningbo Institute of Material Technology and Engineering, Chinese Academy of Sciences, Ningbo 315201, PR China
[b] Harbin Institute of Technology, Harbin 150001, PR China
[c] Lanzhou University of Technology, Lanzhou 730050, PR China

ARTICLE INFO

Article history:
Received 5 January 2013
Received in revised form 30 January 2013
Accepted 26 February 2013
Available online 5 March 2013

Keywords:
Chitin nanocrystals
Acetylation
Surface modification
PHBV

ABSTRACT

Acetylated chitin nanocrystals were prepared through surface modification, and biodegradable poly (3-hydroxybutyrate-co-3-hydroxyvalerate) (PHBV)/chitin nanocrystals films were produced via solution-casting method. Transmission electron microscopy observations and X-ray diffraction profiles revealed that the rod-like morphology and crystal structure of chitin nanocrystals were maintained. Fourier transform infrared spectroscopy and X-ray photoelectron spectroscopy results showed that the hydroxyl groups were partly replaced by the acetyl groups on the surface of chitin nanocrystals. The hydrophobic performance of the acetylated chitin nanocrystals was significantly increased according to the contact angle measurements. Differential scanning calorimeter results indicated that the influence of chitin nanocrystals on the crystallization behaviors of PHBV matrix was changed from suppression to assistance after the surface modification. Tensile test showed that the tensile strength and Young's modulus of PHBV/acetylated chitin nanocrystals composites were improved by 44% and 67%, comparing to the improvement of 24% and 43% for PHBV/chitin nanocrystals composites with the addition of 5.0 wt.% nanocrystals into PHBV.

1. Introduction

Renewable natural nanocrystals derived from natural polysaccharides, such as chitin, starch, and cellulose, have attracted great attention owing to their distinct biocompatibility and biodegradability (Habibi & Dufresne, 2008). They all have high surface area and high Young's modulus (Sturcova, Davies, & Eichhorn, 2005), which makes them suitable candidates for polymer reinforcement (Dufresne, 2008, 2012; Lin, Huang, & Dufresne, 2012; Samir, Alloin, & Dufresne, 2005). Chitin, the most abundant natural amino polysaccharide, is mainly produced from shrimp, crap, tortoise, and insects (Zeng, He, Li, & Wang, 2012). In previous studies, chitin nanofibrils have been used to reinforce both non-biodegradable and biodegradable polymers, such as natural rubber (Nair & Dufresne, 2003), poly(S-co-BuA) (Paillet & Dufresne, 2001), poly (vinyl alcohol) (Junkasem, Rujiravanit, & Supaphol, 2006), polycaprolactone (PCL) (Morin & Dufresne, 2002), raw silk fiber (Wongpanit et al., 2007), chitosan (Sriupayo, Supaphol, Blackwell, & Rujiravanit, 2005), starch (Chang, Jian, Yu, & Ma, 2010) and soy protein isolate (Lu, Weng, & Zhang, 2004). In addition, Chitin nanofibrils are considered to have great potential for applications in tissue engineering scaffolds, drug delivery, and wound dressing (Azuma et al., 2012; Muzzarelli & Muzzarelli, 2005; Muzzarelli et al., 2007; Muzzarelli, 2012).

However, like all the other polysaccharide nanoparticles, the polar hydroxyl groups on the chitin nanocrystals weaken the interfacial interaction which inhibits the positive function of the polysaccharide nanocrystals in many kinds of nonpolar and weak polar polymer matrices (Yuan, Nishiyama, Wada, & Kuga, 2006). Surface chemical modification is an effective method to increase the applications of polysaccharide nanocrystals and lots of relevant research works have been done. In the recent years, it has been reported that some lipophilic chains, such as stearic acid chloride (Thielemans, Belacem, & Dufresne, 2006), poly (tetrahydrofuran) (Labet, Thielemans, & Dufresne, 2007) and PCL (Feng et al., 2009), were used to chemically modify the properties of polysaccharide nanocrystals. By the introduction of hydrophobic functional groups instead of the hydrophilic hydroxyl groups on chitin nanocrystals, it is expected that the dispersibility into nonpolar solvents and

* Corresponding author. Tel.: +86 574 87911135; fax: +86 574 86685186.
** Corresponding author.
E-mail addresses: guqun@nimte.ac.cn (Q. Gu), wangzb@nimte.ac.cn (Z. Wang).

0144-8617/$ – see front matter © 2013 Elsevier Ltd. All rights reserved.
http://dx.doi.org/10.1016/j.carbpol.2013.02.055

adhesion properties with hydrophobic matrices will be improved. Feng et al. (2009) synthesized chitin whisker-graft-polycaprolacton (CHW-g-PCL) by initiating the ring-open polymerization of caprolactone monomer onto the chitin whisker surface. The results showed that the process of grafting PCL chains destroyed the original rod-like structure of chitin nanocrystals, so the tensile strength and the breaking elongation of the nanocomposites were decreased with the increase of chitin whisker content in CHW-g-PCL. Chen et al. reported similar results that the original structure of the cellulose nanocrystals was destroyed by the grafting polymer chains (Chen, Dufresne, Huang, & Chang, 2009).

PHBV is a semicrystalline copolymer which can be produced by bacterial fermentation with *Alcaligenes eutrophus* from renewable natural materials (Kamiya, Yamamoto, Inoue, Chujo, & Doi, 1989). Because of the excellent biodegradability and biocompatibility, PHBV has recently attracted considerable attention by scientists and engineers. However, the disadvantages such as brittleness, poor thermal and mechanical properties restrict its wider utilities. These disadvantages are caused by the comparatively low crystallization nucleation density and slow crystallization rate (Li, Lai, & Liu, 2004). Great efforts have been made to overcome these disadvantages. The addition of nanoparticles as nucleating agents has become attractive because the nanoparticles are not only useful in nucleating the polymer but also beneficial to thermal and mechanical properties of the composites. It has been reported that organophilic montmorillonite (Wang et al., 2005), organoclay (Choi, Kim, Park, Chang, & Lee, 2003), carbon nanotubes (Ma et al., 2012), fumed silica (Ma et al., 2008) and cellulose nanowhiskers (Tena, Jiang, & Wolcott, 2013) were used in PHBV matrix as reinforcing agents.

Since PHBV/polysaccharide nanocrystals nanocomposites are composed of fully biodegradable polymer components, these bionanocomposites have received an increasing interest over the last decades. In our previous works, chitin nanocrystals-graft-PHBV was prepared as nucleation agent in PHBV matrix (Wang et al., 2012). However, the modified nanocrystals did not assist the crystallization behavior of PHBV. These results showed that the crystallization behavior of PHBV was suppressed at the present of chitin nanocrystals and modified chitin nanocrystals. The result might be attributed to the intermolecular hydrogen bonds between the PHBV carbonyls groups and the chitin hydroxyls groups, which restricted the mobility of polymer chains (Ikejima, Yagi, & Inoue, 1999).

In this paper, a simple method was used to prepare hydrophobic chitin nanocrystals which introduced the acetyl groups onto the surface of chitin nanocrystals and maintained the morphology and crystal structure of original chitin nanocrystals. We found that the modified nanofibrils assisted the crystallization behavior of PHBV and reinforced the strength properties comparing to the original chitin nanocrystals.

2. Experimental

2.1. Materials

Chitin from shrimp shells was purchased from Aladdin reagent Co., Ltd. (Shanghai, China). Chitin nanocrystals were prepared through acid hydrolysis as described in previous report (Paillet & Dufresne, 2001). PHBV containing 40% molar hydroxyvalerate (HV) monomer was supplied by Tianan Biologic Co., Ltd. (Ningbo, China). The weight average molecular weight (M_w) was approximately 370 kDa, determined by gel-permeation chromatography (GPC) using polystyrene as standard sample. PHBV with low molecular weight was prepared by acid degradation. After degradation, the M_w was reduced to 35 kDa with the PDI of 2.2 as determined by GPC. Hydrochloric acid, potassium hydroxide, succinic acid, p-toluenesulfonic acid, dimethyl sulfoxide, glacial acetic acid, acetic anhydride, methanesulphonic acid and absolute ethyl alcohol were purchased from Sinopharm Chemical Reagent Co., Ltd. (Shanghai, China). All reagents were used as received without further purification.

2.2. Preparation of acetylated chitin nanocrystals

Chitin nanocrystals were used after vacuum-dried 12 h. 0.5 g of the chitin nanocrystals and 30 ml of glacial acetic acid were placed in a 250 ml three-neck flask. Subsequently, the resultant suspension was treated under ultrasonic conditions for 10 min. After the ultra-sonication, 60 ml of acetic anhydride was added to the mixture followed by stirring for 5 min. 0.1 g of methanesulphonic acid was added to the reactor and the reaction mixture was stirred for the desired time at 45 °C. After modification, the suspension was centrifuged and the precipitation was washed with absolute ethyl alcohol for three times. Then the precipitation was dispersed into absolute ethyl alcohol for producing acetylated chitin nanocrystals suspension. Acetylated chitin nanocrystals suspension was dialyzed against several changes of absolute ethyl alcohol. Two kinds of acetylated chitin nanocrystals with different degrees of substitution were prepared by controlling the reaction time for 20 min and 60 min. For brevity, they were named as acetylated chitin nanocrystals-1 and acetylated chitin nanocrystals-2, respectively, in this work from now on.

2.3. Fabrication of PHBV/chitin nanocrystals films

PHBV/chitin nanocrystals films with various chitin nanocrystals concentrations of 1.0, 3.0 and 5.0 wt.% were prepared via a solution-casting method. 6.0 wt.% PHBV was dissolved in the chloroform at 40 °C. Chitin nanocrystals were added into the PHBV solution and ultrasonic in an ultrasonic bath for 1 h. After that, the mixture was smeared onto a clean glass surface and evaporated overnight at room temperature. The films were subsequently dried in the vacuum oven at 40 °C for 24 h. The neat PHBV film was also prepared according to the same procedure in the absence of chitin nanocrystals in order to eliminate experimental error. All films were kept in a desiccator containing allochroic silicagel at room temperature for 1 week prior to any test.

2.4. Instrumental analysis

Transmission electron microscopy (TEM) images of chitin nanocrystals and acetylated chitin nanocrystals were obtained on an FEI Tecnai G2 F20 transmission electron microscopy with an accelerating voltage of 200 kV. Chitin nanocrystals were dispersed in a 0.5% ethyl alcohol solution. A drop of the solution was introduced on a carbon-coated copper grid without any sample staining.

Wide angle X-ray diffraction (WAXD) patterns were recorded on a Bruker D8 diffractometer, using Ni-filtered Cu Kα radiation at 40 kV and 30 mA at room temperature in an angle ranged from 5° to 40° at a rate of 3.5°/min.

Fourier transform infrared (FTIR) spectra were recorded using a Nicolet 6700 spectrometer. The chitin nanocrystals and acetylated chitin nanocrystals samples were collected using the KBr pellet method. The resolution was 4 cm^{-1} in the range from 400 to 4000 cm^{-1} and the total scans were 32. The samples were dried in the vacuum oven at 100 °C for 24 h before measurement.

X-ray photoelectron spectroscopy (XPS) experiments were carried out using AXIS UTLTRADLD (Shimadzu Corporation, Japan), operated at 15 kV under a current of 30 mA. Samples were placed in an ultrahigh vacuum chamber with electron collection. Relative

atomic concentrations were determined by subtracting a Shirley-type background.

Contact angle measurements were performed at room temperature using Dataphysics OCA20 Contact Angle System. Two different liquids, with different dispersive and polar surface tensions, were used to determine the surface energy of the chitin nanocrystals. Liquid drops were dropped at the speed of 0.1 μl/s onto the pellets. The pellets with smooth surface were obtained by pressing chitin nanocrystals on a tablet machine. Contact angle measurements were carried out on chitin nanocrystals samples before and after surface modification.

Differential scanning calorimetry (DSC) measurements were performed with a Mettler Toledo DSC under nitrogen atmosphere. The samples of neat PHBV and PHBV/chitin nanocrystals films were first heated to 190 °C at a heating rate of 40 °C/min (first heating), and equilibrated at 190 °C for 3 min to remove the thermal history. Subsequently, the samples were cooled to −30 °C at a scanning rate of 10 °C/min (first cooling). Finally, the samples were reheated to 190 °C at a heating rate of 10 °C/min (second heating).

Tensile test of PHBV/chitin nanocrystals films was performed on an Instron 5567 at a tensile rate of 5 mm/min. Dumbbell-shape film specimens were prepared with a Type IV sample cutter. In all cases, ten samples were measured and the mean and standard deviation were calculated.

3. Results and discussion

3.1. TEM

The morphologies of the original chitin nanocrystals (a) and acetylated chitin nanocrystals (b) were observed using TEM (Fig. 1). Fig. 1a shows that the morphology of chitin nanocrystals obtained after acid hydrolysis is rod like in shape with sharp points, which is almost the same as reported previously (Junkasem et al., 2006; Nair & Dufresne, 2003). The length of chitin nanocrystals is 150–400 nm and the width is 20–40 nm. The nanocrystals slightly bonded as a result of hydrogen interactions via the surface hydroxyl groups. The morphology of the surface chemical modified chitin nanocrystals by acetic anhydride is shown in Fig. 1b. The rod-like morphology of the nanocrystals does not change after chemical modification. However, the outlines of the acetylated chitin nanocrystals are blurred and their average length and width decrease slightly. These changes can be attributed to that the low ordered regions on the surface of the chitin nanocrystals are slightly hydrolyzed and dissolved in the acetic acid solution (Borch, Sarko, & Marchessault, 1972). Moreover, the aggregation degree of the acetylated chitin nanocrystals appears to be reduced after modification (Fig. 1b). It might be attributed to that the intermolecular hydrogen bond interactions between the surface hydroxyl groups reduced after the surface modification (Xu et al., 2010).

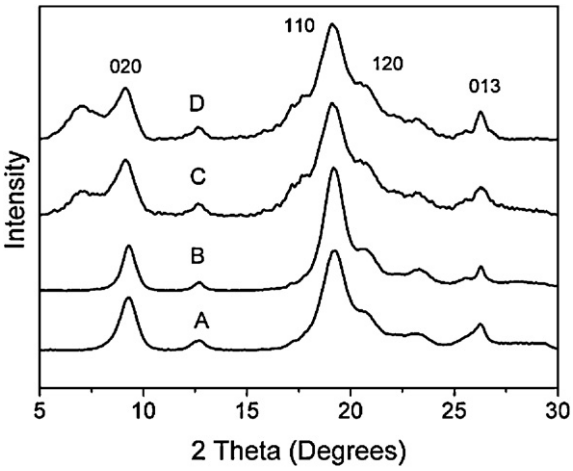

Fig. 2. WAXD patterns of shrimp chitin (A), chitin nanocrystals (B), acetylated chitin nanocrystals-1 (C) and acetylated chitin nanocrystals-2 (D).

3.2. WAXD

WAXD was used to study the crystal structure of original chitin, chitin nanocrystals and acetylated chitin nanocrystals. As shown in Fig. 2, all the chitin nanocrystals, as well as the original chitin, have diffraction peaks at 9.2°, 19.3°, 20.7° and 26.3°, which are typical for the α-chitin structure (Minke & Blackwell, 1978). Hence, the original α-chitin structure was maintained after the acid hydrolysis process and the acetylated reaction. However, the acetylated chitin nanocrystals show a diffraction peak at 7.2° and a small shoulder peak at 17.7°, which are the typical pattern of chitin diacetate (Kim, Nishiyama, & Kuga, 2002). This profile clearly shows that chitin nanocrystals are acetylated heterogeneously from the surface to the core. The crystallinity of the pure shrimp chitin, chitin nanocrystals, acetylated chitin nanocrystals-1 and acetylated

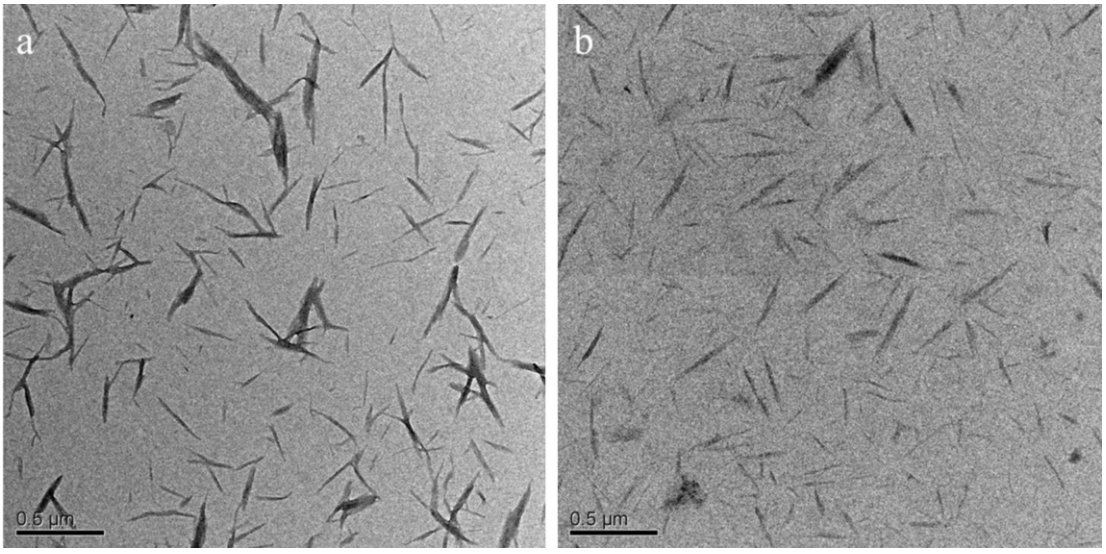

Fig. 1. TEM images of chitin nanocrystals (a) and acetylated chitin nanocrystals-2 (b).

chitin nanocrystals-2 were measured to be 64%, 84%, 78% and 76%, respectively.

3.3. FTIR

FTIR spectra of the chitin nanocrystals and acetylated chitin nanocrystals are shown in Fig. 3. Compared to the chitin nanocrystals, the acetylated chitin nanocrystals show an obvious ester signal at 1742 cm^{-1}, and the intensity of the ester bands gradually become stronger with the increase of reaction time. In addition, the band at 1385 cm^{-1}, which is undoubtedly the CH_3 symmetrical deformational mode, is greatly strengthened in the spectra of the acetylated chitin nanocrystals, the results above indicate that the acetyl groups were introduced into the chitin nanocrystals. At the same time, new absorption band at 1240 cm^{-1} could be assigned to the stretching of ether groups (C—O—C) resulted from the acetylated reaction. The appearance of these new absorptions suggests that the acetylated chitin nanocrystals were formed during the chemical modification process. The absorption bands at 1659 cm^{-1} and 1558 cm^{-1} are attributed to the amide I band and amide II band which are the characteristic absorptions of chitin (Pearson, Marchessault, & Liang, 1960). The amide I band at 1659 cm^{-1} which can be attributed to the stretching of C=O groups hydrogen bonded to NH groups of the neighboring chain has no obviously changed after the modification. This result means that the amide groups were maintained in the acetylated modification. Interestingly, the band at 1621 cm^{-1}, which is assigned to intermolecular hydrogen bonds between CH_3 and OH-6 groups of the adjacency units in the same chains (Focher, Naggi, Torri, Cosani, & Terbojevich, 1992; Pearson et al., 1960), is gradually weakened with the increase of reaction time. The reason may be that the hydroxyl groups including OH-6 reacted with the acetic acid resulting to the broken of intermolecular hydrogen bonds. Meanwhile, the OH stretching at the 3480 cm^{-1} is slightly weakened after the acetylated modification, but the peak still exists. The reason might be that the modification is just occurred on the surface of the chitin nanocrystals, and amounts of hydroxyl groups still exist in the core of chitin nanocrystals.

3.4. XPS

X-ray photoelectron spectroscopy, like elemental analysis, can provide more quantitative measurement than FTIR, so it was used to investigate changes of element composition on the surface of the chitin nanocrystals. The full XPS spectra for both chitin nanocrystals and acetylated chitin nanocrystals are shown in Fig. 4a. The signals observed around binding energies of 532, 398 and 286 eV correspond to the 1s orbital electrons of oxygen, nitrogen and carbon, respectively. The surface elemental compositions are summarized in Table 1. Carbon, nitrogen and oxygen atoms are main components in both chitin nanocrystals and acetylated chitin nanocrystals. The ratio of oxygen-to-carbon for both chitin nanocrystals and acetylated chitin nanocrystals are almost 0.5, because the ratio of oxygen-to-carbon for acetyl groups, similar to the unmodified chitin nanocrystals, is also 0.5. The nitrogen content gradually decreases after modification, while both the oxygen and carbon contents increase, since the acetyl groups replaced the hydrogen atoms in the acetylated modification process.

The deconvolutions of the C 1s signals of chitin nanocrystals and acetylated chitin nanocrystals are shown in Fig. 4b and c, and their binding energies and relative atomic percentages are summarized in Table 1. Four different types of carbon with different chemical environments are observed in the nanocrystals, which are assigned to C1 (C—C/C—H), C2 (C—O/C—N), C3 (O—C—O/C=O) and C4 (O—C=O), respectively. In this case, the C1 (C—C/C—H) and C4 (O—C=O) contributions increase obviously for the presence of the acetyl groups because of surface modification. Meanwhile, the C2 (C—O/C—N) and C3 (O—C—O/C=O) contributions decrease for the acetyl groups contained higher ratio of alkyl groups and ester groups. All of these evolutions in the deconvolutions of main carbon signals give additional evidence of modification efficiency. The C4 contribution gradually increases with reaction time. This result accords with the conclusion obtained from FTIR.

3.5. Contact angle measurements

Contact angle measurements were conducted to provide information of surface tension and wettability of the chitin nanocrystals using water and hydrophobic diiodomethane liquid droplets. Table 2 shows the contact angle (θ) values of chitin nanocrystals and acetylated chitin nanocrystals. The θ value with water of chitin nanocrystals is 31°, while that of the acetylated chitin nanocrystals increase to 61° and 68°, because the hydroxyl groups of the chitin nanocrystals are partly replaced by acetyl groups on the surface of acetylated chitin nanocrystals. Correspondingly, the θ value with diiodomethane decreases from 51° to 39° and 36° after the modification (Table 2). As a result, the increase of the surface hydrophobicity provides additional evidence of the acetylated modification, which agrees with the results of FTIR and XPS investigations.

3.6. DSC

DSC curves of cooling and second heating scans of neat PHBV, PHBV/chitin nanocrystals films are shown in Fig. 5. The crystallization temperature (T_c) shifts to low temperature and the cool

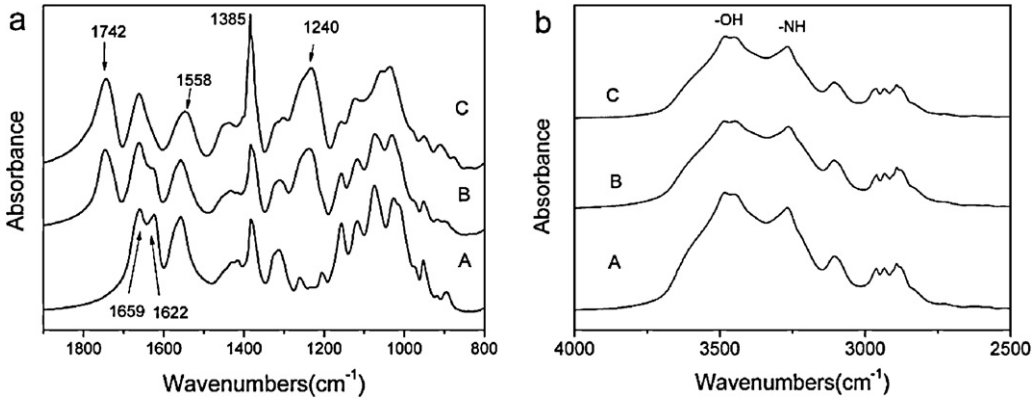

Fig. 3. FTIR spectra of chitin nanocrystals (A), acetylated chitin nanocrystals-1 (B) and acetylated chitin nanocrystals-2 (C).

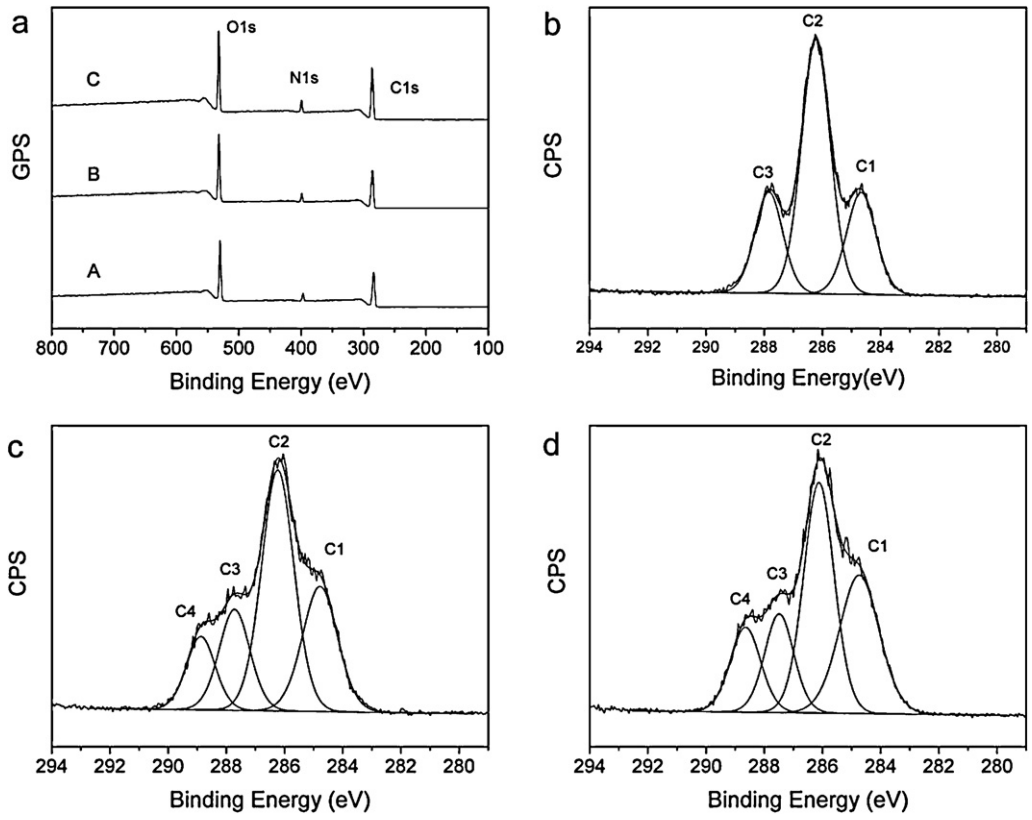

Fig. 4. Full XPS spectra (a) of the chitin nanocrystals (A), acetylated chitin nanocrystals-1 (B) and acetylated chitin nanocrystals-2 (C) and the deconvolutions of the C 1s signal into its constituent contributions for chitin nanocrystals (b), acetylated chitin nanocrystals-1 (c) and acetylated chitin nanocrystals-2 (d).

Table 1
Elemental surface compositions of chitin nanocrystals and acetylated chitin nanocrystals, determined by XPS, and surface functional groups compositions from the deconvolutions of the C 1s signals with average binding energy position.

Sample	Elemental analysis (%)			Composition of C in groups (%)			
	O	C	N	C1 (C—C/C—H)	C2 (C—O/C—N)	C3 (O—C—O/C=O)	C4 (O—C=O)
Binding energy (eV)	532	286	398	284.4	286.1	287.8	288.6
Chitin nanocrystals	31.2	62.3	6.5	22.9	55.2	21.9	N/A
Acetylated chitin nanocrystals-1	31.3	62.5	6.2	25.2	44.9	17.8	12.1
Acetylated chitin nanocrystals-2	31.5	63.2	5.4	30.6	39.1	15.9	14.4

crystallization temperature (T_{cc}) rises with the addition of 1.0 wt.% unmodified chitin nanocrystals. These results indicate that the crystallization of PHBV is suppressed with the present of chitin nanocrystals. This is due to that the hydrogen bonds between the PHBV carbonyls and the chitin hydroxyls could confine the diffusion and migration of polymer chains (Chen, Zhou, Zhuang, & Dong, 2005; Ikejima et al., 1999).

However, the T_c of the composites with the addition of 1.0 wt.% acetylated chitin nanocrystals-2 is approximately 5 °C higher than neat PHBV. In contrast to the unmodified chitin nanocrystals, acetylated chitin nanocrystals assist the nonisothermal melt crystallization of the PHBV matrix. This conclusion can also be proved by Fig. 5b in which both the T_{cc} values of PHBV/acetylated chitin nanocrystals films shift to lower temperature compared with neat PHBV and PHBV/chitin nanocrystals films. The reason is that the hydrogen bonds between the PHBV carbonyls and the chitin hydroxyls decrease sufficiently, which have been confirmed by the results of FTIR, XPS and contact angle.

Table 2
Contact angle (θ) values of chitin nanocrystals and acetylated chitin nanocrystals.

Sample	θ	
	Water	Diiodomethane
Chitin nanocrystals	31°	51°
Acetylated chitin nanocrystals-1	61°	39°
Acetylated chitin nanocrystals-2	68°	36°

3.7. Tensile test

The addition of polysaccharide nanocrystals may result in the improvement in mechanical properties of polymer matrix, because the intrinsic strength of polysaccharide nanocrystals is much excellent (Cao, Dong, & Li, 2007; Kadokawa, Takegawa, Mine, & Prasad, 2011; Tena, Turtle, Bahr, Jiang, & Wolcott, 2010). Tensile strength and Young's modulus of neat PHBV and PHBV/chitin nanofibrils films are shown in Fig. 6. The addition of the chitin nanofibrils and the acetylated chitin nanofibrils significantly enhanced the ultimate tensile strength and Young's modulus of the PHBV matrix. Compared with the neat PHBV, the ultimate tensile strength and Young's modulus of PHBV are improved by about 24% and 43%, respectively, with the incorporation of 5.0 wt.% chitin nanofibrils. However, with the addition of 5.0 wt.% acetylated chitin nanofibrils, the ultimate tensile strength and Young's modulus of PHBV are improved by 44% and 67%, respectively. This result indicates

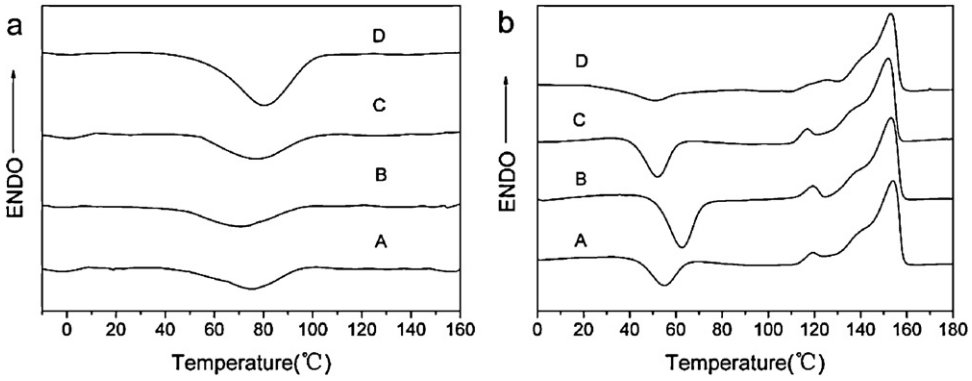

Fig. 5. DSC curves of neat PHBV and PHBV/chitin nanocrystals films from the cooling (a) and second heating (b) scans with various chitin nanocrystals: (A) neat PHBV, (B) 1.0 wt.% chitin nanocrystals, (C) 1.0 wt.% acetylated chitin nanocrystals-1 and (D) 1.0 wt.% acetylated chitin nanocrystals-2.

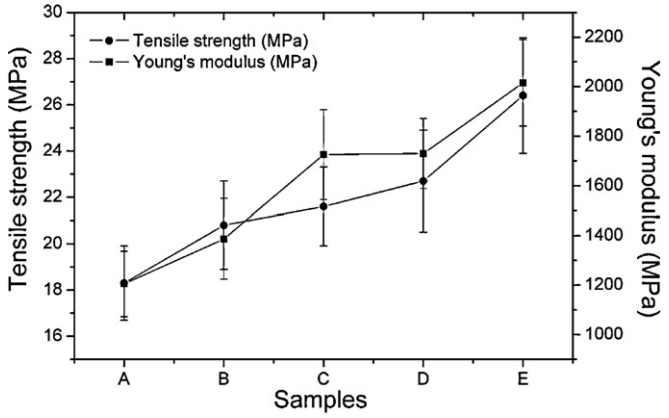

Fig. 6. Tensile strength and Young's modulus of neat PHBV (A) and PHBV/chitin nanofibrils films with various chitin nanofibrils: (B) 3.0 wt.% chitin nanofibrils, (C) 3.0 wt.% acetylated chitin nanofibrils-2, (D) 5.0 wt.% chitin nanofibrils and (E) 5.0 wt.% acetylated chitin nanofibrils-2.

that the acetylated chitin nanofibrils have more effective influence on the mechanical properties of the PHBV matrix than the original chitin nanofibrils. The reason may be that the acetylated chitin nanofibrils have better dispersion than the original chitin nanofibrils in the weak polar PHBV matrix.

4. Conclusions

To concluded, acetylated chitin nanocrystals remained the rod-like morphology and crystal structure compared with original chitin nanocrystals, and that the hydrophilic hydroxyl groups were partly replaced by acetyl groups on the surface of chitin nanocrystals. Moreover, the hydrophobicity of chitin nanocrystals was improved by the introduction of hydrophobic acetyl groups. Since acetylated modification reduced the intermolecular hydrogen bonds between PHBV matrix and chitin nanocrystals, acetylated chitin nanocrystals assisted the crystallization behavior and reinforced the mechanical properties comparing to the original chitin nanocrystals in the weak polar PHBV matrix. This research is expected to be helpful for the investigation and production of polymer/nanocrystals composites.

Acknowledgements

This research was supported by Natural Science Foundation of China (Grant No. 51273207), Program for Ningbo Innovative Research Team (2009B21008), Ningbo Key Lab of Polymer Materials (Grant No. 2010A22001).

References

Azuma, K., Osaki, T., Ifuku, S., Saimoto, H., Tsuka, T., Imagawa, T., et al. (2012). α-Chitin nanofibrils improve inflammatory and fibrosis responses in inflammatory bowel disease mice model. *Carbohydrate Polymers*, *90*, 197–200.

Borch, J., Sarko, A., & Marchessault, R. H. (1972). Light scattering analysis of starch granules. *Journal of Colloid and Interface Science*, *41*, 574–587.

Cao, X. D., Dong, H., & Li, C. M. (2007). New nanocomposite materials reinforced with flax cellulose nanocrystals in waterborne polyurethane. *Biomacromolecules*, *8*, 899–904.

Chang, P. R., Jian, R. J., Yu, J. G., & Ma, X. F. (2010). Starch-based composites reinforced with novel chitin nanoparticles. *Carbohydrate Polymers*, *80*, 420–425.

Chen, C., Zhou, X. S., Zhuang, Y. G., & Dong, L. S. (2005). Thermal behavior and intermolecular interactions in blends of poly(3-hydroxybutyrate) and maleated poly(3-hydroxybutyrate) with chitosan. *Journal of Polymer Science Part B: Polymer Physics*, *43*, 35–47.

Chen, G. J., Dufresne, A., Huang, J., & Chang, P. R. (2009). A novel thermoformable bionanocomposite based on cellulose nanocrystal-graft-poly(ε-caprolactone). *Macromolecular Materials and Engineering*, *294*, 59–67.

Choi, W. M., Kim, T. W., Park, O. O., Chang, Y. K., & Lee, J. W. (2003). Preparation and characterization of poly(hydroxybutyrate-co-hydroxyvalerate)-organoclay nanocomposites. *Journal of Applied Polymer Science*, *90*, 525–529.

Dufresne, A. (2008). Polysaccharide nanocrystal reinforced nanocomposites. *Canadian Journal of Chemistry*, *86*, 484–494.

Dufresne, A. (2012). Polymer nanocomposites reinforced with polysaccharide nanocrystals. *International Journal of Nanotechnology*, *8*, 795–805.

Feng, L. D., Zhou, Z. Y., Dufresne, A., Huang, J., Wei, M., & An, L. J. (2009). Structure and properties of new thermoforming bionanocomposites based on chitin whisker-graft-polycaprolactone. *Journal of Applied Polymer Science*, *112*, 2830–2837.

Focher, B., Naggi, A., Torri, G., Cosani, A., & Terbojevich, M. (1992). Structural differences between chitin polymorphs and their precipitates from solutions-evidence from CP-MAS ^{13}C NMR, FT-IR and FT-Raman spectroscopy. *Carbohydrate Polymers*, *17*, 97–102.

Habibi, Y., & Dufresne, A. (2008). Highly filled bionanocomposites from functionalized polysaccharide nanocrystals. *Biomacromolecules*, *9*, 1974–1980.

Ikejima, T., Yagi, K., & Inoue, Y. (1999). Thermal properties and crystallization behavior of poly(3-hydroxybutyric acid) in blends with chitin and chitosan. *Macromolecular Chemistry and Physics*, *200*, 413–421.

Junkasem, J., Rujiravanit, R., & Supaphol, P. (2006). Fabrication of α-chitin whisker-reinforced poly(vinyl alcohol) nanocomposite nanofibres by electrospinning. *Nanotechnology*, *17*, 4519–4528.

Kadokawa, J., Takegawa, A., Mine, S., & Prasad, K. (2011). Preparation of chitin nanowhiskers using an ionic liquid and their composite materials with poly(vinyl alcohol). *Carbohydrate Polymers*, *84*, 1408–1412.

Kamiya, N., Yamamoto, Y., Inoue, Y., Chujo, R., & Doi, Y. (1989). Microstructure of bacterially synthesized poly(3-hydroxybutyrate-co-3-hydroxyvalerate). *Macromolecules*, *22*, 1676–1682.

Kim, D. Y., Nishiyama, Y., & Kuga, S. (2002). Surface acetylation of bacterial cellulose. *Cellulose*, *9*, 361–367.

Labet, M., Thielemans, W., & Dufresne, A. (2007). Polymer grafting onto starch nanocrystals. *Biomacromolecules*, *8*, 2916–2927.

Li, J., Lai, M. F., & Liu, J. J. (2004). Effect of poly(propylene carbonate) on the crystallization and melting behavior of poly(β-hydroxybutyrate-co-β-hydroxyvalerate). *Journal of Applied Polymer Science*, *92*, 2514–2521.

Lin, N., Huang, J., & Dufresne, A. (2012). Preparation, properties and applications of polysaccharide nanocrystals in advanced functional nanomaterials: A review. *Nanoscale*, *4*, 3274–3294.

Lu, Y. S., Weng, L. H., & Zhang, L. N. (2004). Morphology and properties of soy protein isolate thermoplastics reinforced with chitin whiskers. *Biomacromolecules*, *5*, 1046–1051.

Ma, P. M., Wang, R. Y., Wang, S. F., Zhang, Y., Zhang, Y. X., & Hristova, D. (2008). Effects of fumed silica on the crystallization behavior and thermal properties of

poly(hydroxybutyrate-co-hydroxyvalerate). *Journal of Applied Polymer Science*, *108*, 1770–1777.
Ma, Y. X., Zheng, Y. D., Wei, G. Y., Song, W. H., Hu, T., Yang, H., et al. (2012). Processing, structure, and properties of multiwalled carbon nanotube/poly(hydroxybutyrate-co-valerate) biopolymer nanocomposites. *Journal of Applied Polymer Science*, *125*, E620–E629.
Minke, R., & Blackwell, J. (1978). The structure of α-chitin. *Journal of Molecular Biology*, *120*, 167–181.
Morin, A., & Dufresne, A. (2002). Nanocomposites of chitin whiskers from Riftia tubes and poly(caprolactone). *Macromolecules*, *35*, 2190–2199.
Muzzarelli, R. A. A. (2012). Nanochitins and nanochitosans, paving the way to eco-friendly and energy-saving exploitation of marine resources. In K. Matyjaszewski, & M. Möller (Eds.), *Polymer Science: A Comprehensive Reference* (p. 153-164). Amsterdam: Elsevier BV.
Muzzarelli, R. A. A., & Muzzarelli, C. (2005). Chitin nanofibrils. In P. K. Dutta (Ed.), *Chitin and Chitosan: Research Opportunities and Challenges*. New Delhi, India: New Age Intl.
Muzzarelli, R. A. A., Morganti, P., Morganti, G., Palombo, P., Palombo, M., Biagini, G., et al. (2007). Chitin nanofibrils/chitosan glycolate composites as wound medicaments. *Carbohydrate Polymers*, *70*, 274–284.
Nair, K. G., & Dufresne, A. (2003). Crab shell chitin whisker reinforced natural rubber nanocomposites. 2. Mechanical behavior. *Biomacromolecules*, *4*, 666–674.
Paillet, M., & Dufresne, A. (2001). Chitin whisker reinforced thermoplastic nanocomposites. *Macromolecules*, *34*, 6527–6530.
Pearson, F. G., Marchessault, R. H., & Liang, C. Y. (1960). Infrared spectra of crystalline polysaccharides. V. Chitin. *Journal of Polymer Science*, *43*, 101–116.
Samir, M. A. S. A., Alloin, F., & Dufresne, A. (2005). Review of recent research into cellulosic whiskers, their properties and their application in nanocomposite field. *Biomacromolecules*, *6*, 612–626.
Sriupayo, J., Supaphol, P., Blackwell, J., & Rujiravanit, R. (2005). Preparation and characterization of α-chitin whisker-reinforced chitosan nanocomposite films with or without heat treatment. *Carbohydrate Polymers*, *62*, 130–136.
Sturcova, A., Davies, G. R., & Eichhorn, S. (2005). Elastic modulus and stress-transfer properties of tunicate cellulose whiskers. *Biomacromolecules*, *6*, 1055–1061.
Tena, E., Turtle, J., Bahr, D., Jiang, L., & Wolcott, M. (2010). Thermal and mechanical properties of poly(3-hydroxybutyrate-co-3-hydroxyvalerate)/cellulose nanowhiskers composites. *Polymer*, *51*, 2652–2660.
Tena, E., Jiang, L., & Wolcott, M. P. (2013). Preparation and properties of aligned poly(3-hydroxybutyrate-co-3-hydroxyvalerate)/cellulose nanowhiskers composites. *Carbohydrate Polymers*, *92*, 206–213.
Thielemans, W., Belacem, M. N., & Dufresne, A. (2006). Starch nanocrystals with large chain surface modifications. *Langmuir*, *22*, 4804–4810.
Wang, S. F., Song, C. J., Chen, G. X., Guo, T. Y., Liu, J., Zhang, B. H., et al. (2005). Characteristics and biodegradation properties of poly(3-hydroxybutyrate-co-3-hydroxyvalerate)/organophilic montmorillonite (PHBV/OMMT) nanocomposite. *Polymer Degradation and Stability*, *87*, 69–76.
Wang, J., Wang, Z. B., Li, J., Wang, B. J., Liu, J., Chen, P., et al. (2012). Chitin nanocrystals grafted with poly(3-hydroxybutyrate-co-3-hydroxyvalerate) and their effects on thermal behavior of PHBV. *Carbohydrate Polymers*, *87*, 784–789.
Wongpanit, P., Sanchavanakit, N., Pavasant, P., Bunaprasert, T., Tabata, Y., & Rujiravanit, R. (2007). Preparation and characterization of chitin whisker-reinforced silk fibroin nanocomposite sponges. *European Polymer Journal*, *43*, 4123–4135.
Xu, Y., Ding, W. Q., Liu, J., Li, Y., Kennedy, J. F., Gu, Q., et al. (2010). Preparation and characterization of organic-soluble acetylated starch nanocrystals. *Carbohydrate Polymers*, *80*, 1078–1084.
Yuan, H. H., Nishiyama, Y., Wada, M., & Kuga, S. (2006). Surface acylation of cellulose whiskers by drying aqueous emulsion. *Biomacromolecules*, *7*, 696–700.
Zeng, J. B., He, Y. S., Li, S. L., & Wang, Y. Z. (2012). Chitin whiskers: An overview. *Biomacromolecules*, *13*, 1–11.